Perfect electromagnetic absorption using graphene and epsilon-near-zero metamaterials

Michaël Lobet, Bruno Majerus, Luc Henrard, and Philippe Lambin*
Department of Physics & Research Group on Carbon Nanostructures (CARBONNAGe), University of Namur, 61 rue de Bruxelles, 5000 Namur, Belgium
(Received 18 April 2016; revised manuscript received 24 May 2016; published 14 June 2016)

The ability of graphene/polymer heterostructures to absorb GHz electromagnetic radiation was recently evidenced both theoretically and experimentally [Batrakov *et al.*, Sci. Rep. **4**, 7191 (2014) and Lobet *et al.*, Nanotechnology **26**, 285702 (2015)]. Maximum absorption was shown to depend solely on refractive indices of incident and emergence media once impedance matching conditions are fulfilled. In this paper, analytical models and numerical simulations are performed for both semi-infinite and finite slab substrate. We evidenced that only three graphene layers separated by a dielectric spacer and an epsilon-near-zero metamaterial as emergence medium allow a perfect absorption for normal incidence. The use of lossless epsilon-near-zero metamaterial prevents radiations to go through the device, because of infinite impedance, and forces them to be totally absorbed in the dissipative medium (graphene). The device is proved to be robust regarding angular incidence up to 45 deg for a semi-infinite epsilon-near-zero metamaterial. The proposed strategy is universal and can be applied to any kind of two-dimensional dissipative materials lying on epsilon-near-zero metamaterial. The proposed absorber does not rely on surface patterning or texturing and hence is more appealing for device applications.

DOI: 10.1103/PhysRevB.93.235424

I. INTRODUCTION

The modern world is bathed in overcrowded electromagnetic (em) radiations in the radio-frequency range. Shielding sensitive electronic devices against radio-frequency interferences and dealing with electromagnetic compatibility issues are then of prime necessity. Consequently, the search for light, thin, broadband, and perfect wave absorbers is one of today's challenges [1]. Metals turn out to be a poor solution since they reflect almost 100% of incoming radiation once the thickness exceeds skin depth and additional reflection leads to more em polution.

Graphene revealed to be a good candidate for efficient absorbers due to its remarkable em properties in the GHz regime related to high and broadband conductivity [2,3]. Furthermore, its mechanical flexibility, resistance to high temperature, or the tunability of its electronic properties by an externally applied electrical field are additional advantages [4].

The conductance of few-layer graphite increases linearly with the number of graphene planes when the coupling between the planes is switched off by stacking the planes randomly [5] or by keeping them a few nanometers away from each other. Experimental techniques to fabricate artificial structures containing up to six layers of graphene separated by thin polymer films have been reported [6,7] and can be applied to any kind of substrate [8]. The thickness of the PMMA spacers can be chosen in the range 200–700 nm. Separating several graphene layers by a dielectric spacer is then a way to control the conductivity of the designed heterostructure.

Since dissipation of energy in a material is directly linked to its conductivity, an optimal number of layers can be derived to achieve maximum absorption [6,9]. Interestingly, the condition to reach this maximum solely depends on the refractive indices of the incident medium and of the emergence medium. Once impedance matching conditions are fulfilled for the incoming radiation, a reduction of the refractive index of the substrate is shown, in this work, to drastically increase the absorption by the graphene-based heterostructure, from $A = 50\%$ for the self-supported case to perfect absorption for a substrate with a vanishingly small refractive index. Such a substrate could be realized using metamaterials. Metamaterials are artificial structured materials at subwavelength scale with strikingly unconventional optical properties, such as negative refraction [10–13], cloaking [14,15], or superlenses [10,16,17]. All those new optical effects are the consequence of manipulation of the refractive index. Since all negative refractive index media are dispersive and since the refractive index is a continuous function of the wavelength, a region of wavelengths do exist where the refractive index is near zero. Those particular metamaterials, called near-zero refractive index metamaterials (NZRI), provide propagation at a low wave number and a relatively low phase variation over a physically long distance [18–21]. In such metamaterial, the phase velocity and the wavelength are quasi-infinite in a specific frequency range. Recently, a slab of epsilon-near-zero (ENZ) metamaterials has been considered for perfect absorption in combination with a perfect electric conductor (PEC) [22–25]. Those absorbers rely on coherent perfect absorption when light couples to a fast wave propagation along the ENZ medium, at oblique incidence only. Using graphene as ENZ has also been proposed for the absorption of TM mode by an enhancement of field intensity [26]. However, this strategy requires a metal grating to couple incident light to ENZ graphene.

The present work uses an ENZ metamaterial as substrate and all em energy is dissipated in only three graphene layers. We first briefly review the electrodynamics of an heterostructure possessing a conducting two-dimensional (2D) material as constituent and derive the conditions for maximal absorption in the case of the device lying on a semi-infinite emergence medium and normal incidence. Numerical rigorous coupled wave analysis (RCWA) numerical simulations [27] support the analytical derivations [28,29]. The physical insight of the benefit of ENZ metamaterial is highlighted. Second,

*philippe.lambin@unamur.be

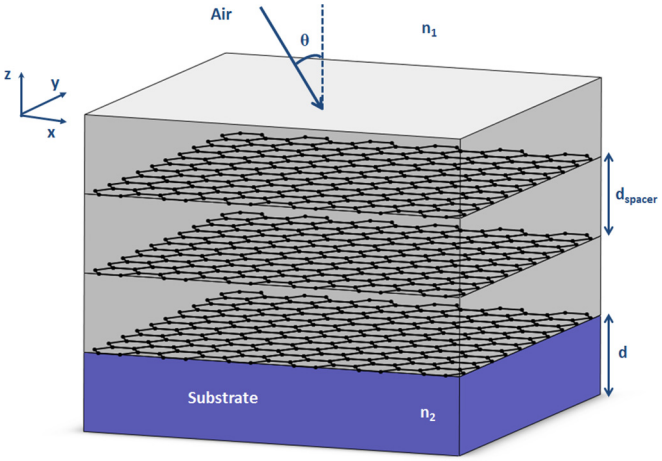

FIG. 1. Electromagnetic radiation impinging on a graphene-PMMA heterostructure composed of three PMMA/graphene units, lying on a substrate of refractive index n_2, with incident angle θ.

an oblique incidence is considered, the formalism for s and p polarizations is presented. Then, a finite slab of ENZ metamaterial is used as substrate. This extra tuning parameter provides a range of optimal thicknesses in agreement with interference theory. Finally, a discussion on the broadband character of the perfectly absorbing device completes the study. The considerations developed here for ENZ metamaterial and 2D materials are totally general and have not been reported yet.

II. ELECTRODYNAMICS OF 2D MATERIAL/POLYMER HETEROSTRUCTURE ON EPSILON-NEAR-ZERO METAMATERIAL

The device is made of alternating 2D conducting sheets, graphene here, sandwiched between poly(methyl methacrylate) (PMMA) thin films [6,9] (Fig. 1). The heterostructure under study proved to be an ultralight shielding material with good mechanical properties [30]. Moreover, absorption properties have been shown, both theoretically and experimentally, to be robust to defects (up to 20%) that may occur during CVD fabrication process. A plane wave with frequency ω is incident on the stratified medium, made of nonmagnetic materials ($\mu = 1$). Those materials are supposed isotropic around the z axis. The operating frequency is assumed, for now, to be 30 GHz ($\lambda = 1$ cm).

Graphene refractive index is linked to its finite 2D conductivity σ_{2D} which obeys a Drude relation up to a few tens of GHz [31–33]:

$$\sigma_{2D} = \frac{e^2}{\pi\hbar^2}\frac{iE_F}{\omega + \frac{i}{\tau}} \tag{1}$$

with τ, the electronic relaxation time [34]. The Fermi energy E_F is related to the doping carrier density n, $E_F = \hbar v_F\sqrt{\pi n}$, where $v_F \approx 1 \times 10^6$ m/s. An experimental determination of graphene sheet conductance to 0.37 in units of $\epsilon_0 c$ at 30 GHz [35] allow us to set the two parameters to $n = 9.1 \times 10^{15}$ m^{-2} and $\tau = 7.5 \times 10^{-14}$ s. The resulting $\sigma_{2D}/\epsilon_0 c$ is equal to $0.37 + 0.007i$, which corresponds to an electronic mobility μ of 6.7×10^3 cm^2/V s. This value agrees with what is known about CVD graphene [36]. The PMMA dielectric spacer possess a purely real dielectric constant of 2.6 [37], while its thickness is arbitrarily fixed to $d_{\text{spacer}} = 700$ nm. This thickness only provides a screening against the van der Waals interaction between adjacent graphene sheets, so it can be made thinner to further reduce size and weight. Nevertheless, the thicknesses of both PMMA and graphene layers are deeply subwavelength at the assumed frequency of the incident radiation. The present heterostructure composed of N graphene/PMMA layers can be modeled as a 2D conducting system with a sheet conductance σ_N equal to N times one of an isolated graphene plane σ_{2D} [5,6], i.e., $\sigma_N = N\sigma_{2D}$. This relation is somehow similar to an effective medium approximation since dimensions of the system are subwavelength. The purely real refractive indices of the incident and emergence media are, respectively, n_1 and n_2. Air is considered as the incident medium, while the nature of the semi-infinite emergence medium will be considered as a parameter in what follows. Solving Maxwell equations with the appropriate boundary conditions leads to the reflectance R and transmittance T at normal incidence [9,33,38]:

$$R = \left|\frac{n_1 - n_2 - \frac{\sigma_N}{\epsilon_0 c}}{n_1 + n_2 + \frac{\sigma_N}{\epsilon_0 c}}\right|^2, \quad T = \frac{4n_1 n_2}{\left|n_1 + n_2 + \frac{\sigma_N}{\epsilon_0 c}\right|^2}. \tag{2}$$

Invoking conservation of energy, the absorption of the 2D conducting layer is

$$A = \frac{4n_1 \mathrm{Re}\left(\frac{\sigma_N}{\epsilon_0 c}\right)}{\left|n_1 + n_2 + \frac{\sigma_N}{\epsilon_0 c}\right|^2}. \tag{3}$$

One readily sees that adjusting the number of graphene layers enables one to tune the absorption of the system. A careful analysis shows that maximum of A reaches the value

$$A_{\max} = \frac{n_1}{n_1 + n_2} \tag{4}$$

upon the conditions

$$\begin{aligned} &\mathrm{Re}\,\sigma_N/\epsilon_0 c = n_1 + n_2, \\ &\mathrm{Im}\,\sigma_N/\epsilon_0 c = 0, \end{aligned} \tag{5}$$

which correspond to impedance matching conditions. It can be noticed that the condition on the imaginary part is fairly fulfilled since the imaginary part of graphene conductance is three orders of magnitude lower than its real part in the considered frequency range. Maximum of absorption will then take place when the conductivity of the graphene/PMMA heterostructure matches the sum of the refractive indices of the incident and emergence media [Eq. (5)]. Previous studies using a 0.5-mm-thick substrate made of SiO_2 (refractive index equals to 1.92) required around seven graphene layers to reach an absorption of 41.8% with air as incidence medium [9].

Since maximum absorption [Eq. (4)] depends solely on the refractive indices of the incident and emergence media, a direct way to reach perfect absorption is to reduce the refractive index of the emergence medium. This kind of consideration perfectly falls into the scope of metamaterials theory. It should be noted that a NZRI requirement for perfect absorption is a too strong condition. Actually, the constitutive equations of electromagnetism provide the relation between the refractive index n, the

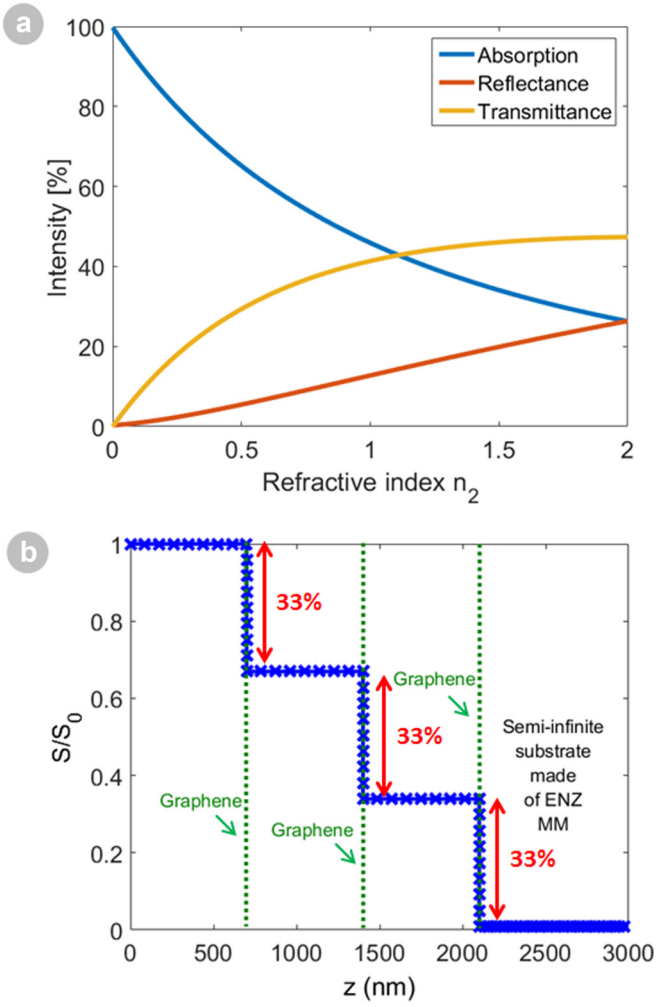

FIG. 2. (a) Absorption (blue), reflectance (red), and transmittance (yellow) of a multilayer composed of three PMMA/graphene units versus the refractive index of the semi-infinite emergence medium at 30 GHz and normal incidence. Absorption increases as the refractive index of the emergence medium vanishes. (b) Normalized Poynting vector versus depth z under normal incidence at 30 GHz for a semi-infinite emergence medium of refractive index equal to 0.01. Absorption occurs only in graphene layers and 1/3 of incident electromagnetic energy is dissipated at each graphene-polymer interface.

electric permittivity ε, and the magnetic susceptibility μ, i.e., $n = \sqrt{\varepsilon\mu}$. Consequently, achieving NZRI requires either ε or μ to approach zero. Since nonmagnetic materials ($\mu = 1$) are considered here, effects of ENZ metamaterials as substrate on 2D materials absorption are investigated.

A vanishing refractive index n_2 for the emergence medium imposes a fewer number of graphene layers according to the above impedance matching conditions [Eq. (5)]. Three layers of graphene (3×0.37) are sufficient to match the refractive index of air. This further reduces the complexity of the graphene stacking.

Slowly decreasing the effective refractive index of the emergence medium boosts the absorption of the shielding device as confirmed by Eqs. (2) and (3) [Fig. 2(a)]. For example, absorption of 98.8% is observed for an effective permittivity of 1×10^{-4} or $n_2 = 0.01$. Simultaneously, reflectance and transmittance are vanishing as $R_{\max} = \frac{|n_2|^2}{|n_1+n_2|^2}$ and $T_{\max} = \frac{n_1 n_2}{|n_1+n_2|^2}$. They both tend to zero with n_2, confirming the perfect absorption. Complementary to the analytical relations presented above, RCWA calculations [27] have been performed to localize the absorption in the device and get information about the fields [28,29]. Absorption occurs only in the graphene layers as shown in Fig. 2(b). The displayed normalized Poynting vector, representing the flow of em energy, is reduced by 1/3 after each graphene layer. The electric field incident upon each graphene layer induces currents which efficiently dissipates the em energy by Joule effect. As a result, transmitted and reflected energies are very low.

One may question the role of the ENZ metamaterial. It is drastically different to what was previously reported for perfect absorption in literature [22–26]. The ENZ metamaterial blocks the em energy, more specifically acts as a magnetic wall. The magnetic field is uniformly zero into the ENZ emergence medium, while the tangential component of the electric field is still significant. With a 2D conducting sheet on top of it, part of the incident energy is dissipated [39]. Since the sum of reflectance and transmittance is minimized due to the impedance matching conditions, all em energy has to disappear in the only dissipative element: the conducting 2D material, i.e., graphene.

Such a magnetic wall can be realized with high impedance substrate [40]. The impedance Z is defined in optics as $Z = \sqrt{\frac{\mu}{\varepsilon}}\mu_0 c$. For ENZ metamaterial, an infinite impedance is derived and it consequently acts as a magnetic wall. This strategy may resemble a Salisbury screen [41], a resistive sheet located a quarter wavelength away from a metallic surface. However, the difference with the Salisbury screen is that here the distance between the dissipative elements and the ENZ metamaterial is not necessarily $\lambda/4$ for a semi-infinite emergence medium and could be made thinner.

III. ANGULAR DEPENDENCE

Once normal incidence is no longer considered, the above relations (2) and (3) and impedance matching conditions (5) depend on the incident angle θ_1 and vary with the polarization. Solving Maxwell equations for both s and p polarizations gives, with θ_1 (θ_2) the incident (refracted) angle,

$$R_s = \left| \frac{\frac{n_1\cos\theta_1 - n_2\cos\theta_2}{2} - \frac{\sigma_N}{2\epsilon_0 c}}{\frac{n_1\cos\theta_1 + n_2\cos\theta_2}{2} + \frac{\sigma_N}{2\epsilon_0 c}} \right|^2, \tag{6}$$

$$T_s = \frac{n_1 n_2 \cos\theta_1 \cos\theta_2}{\left| \frac{n_1\cos\theta_1 + n_2\cos\theta_2}{2} + \frac{\sigma_N}{2\epsilon_0 c} \right|^2}, \tag{7}$$

$$A_s = \frac{n_1\cos\theta_1 \mathrm{Re}\left(\frac{\sigma_N}{\epsilon_0 c}\right)}{\left| \frac{n_1\cos\theta_1 + n_2\cos\theta_2}{2} + \frac{\sigma_N}{2\epsilon_0 c} \right|^2}, \tag{8}$$

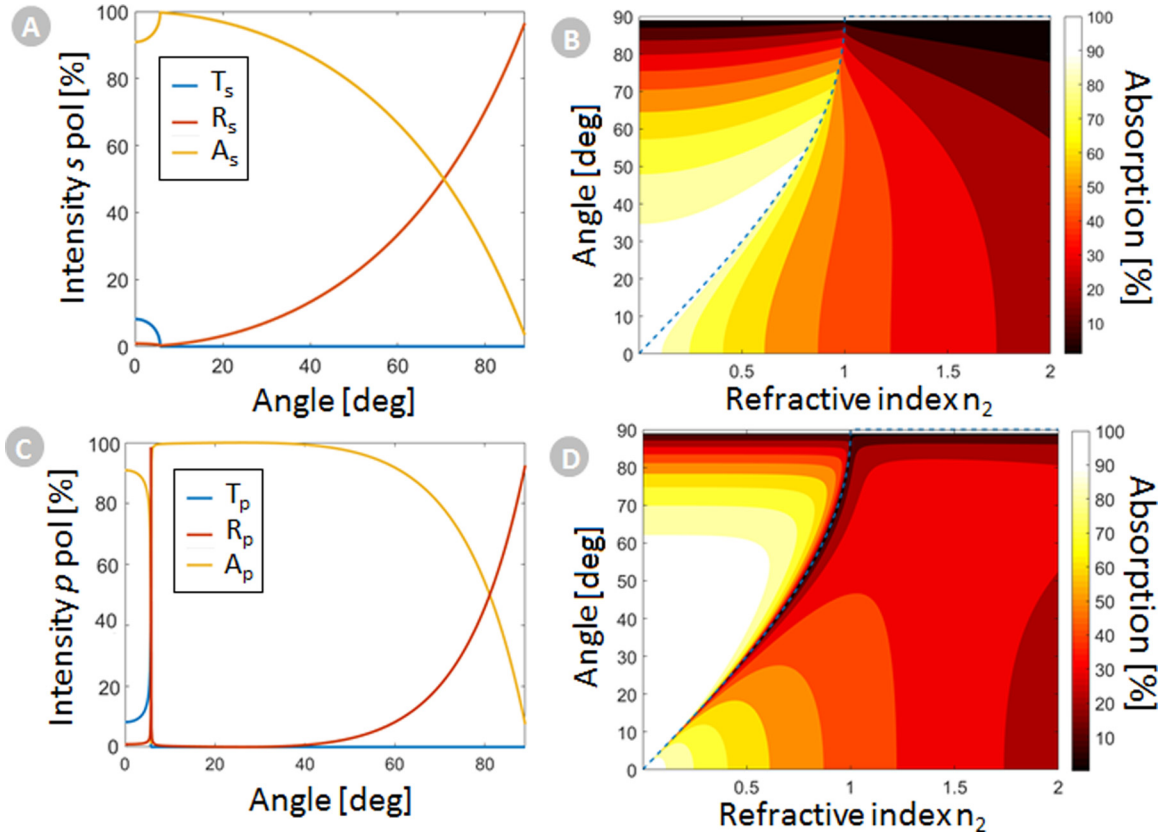

FIG. 3. (a) Transmittance (blue), reflectance (red), and absorption (yellow) for s polarization of a multilayer composed of three PMMA/graphene units versus angle of incidence of the semi-infinite emergence medium at 30 GHz and $n_2 = 0.1$. (b) Absorption map in s polarization for emergence medium refractive index varying from 0.001 to 2 and incidence angle from 0 to 89 deg. The dotted blue line corresponds to critical angle θ_L. (c) Transmittance (blue), reflectance (red), and absorption (yellow) for p polarization of a multilayer composed of three PMMA/graphene units versus angle of incidence of the semi-infinite emergence medium at 30 GHz and $n_2 = 0.1$. (d) Absorption map in p polarization for emergence medium refractive index varying from 0.001 to 2 and incidence angle from 0 to 89 deg. The dotted blue line corresponds to critical angle θ_L.

and

$$R_p = \left| \frac{\frac{n_1\cos\theta_2 - n_2\cos\theta_1}{2} - \frac{\sigma_N}{2\epsilon_0 c}\cos\theta_1\cos\theta_2}{\frac{n_1\cos\theta_2 + n_2\cos\theta_1}{2} + \frac{\sigma_N}{2\epsilon_0 c}\cos\theta_1\cos\theta_2} \right|^2, \tag{9}$$

$$T_p = \frac{n_1 n_2 \cos\theta_1\cos\theta_2}{\left|\frac{n_1\cos\theta_2 + n_2\cos\theta_1}{2} + \frac{\sigma_N}{2\epsilon_0 c}\cos\theta_1\cos\theta_2\right|^2}, \tag{10}$$

$$A_p = \frac{n_1\cos\theta_1\cos^2\theta_2 \mathrm{Re}\left(\frac{\sigma_N}{\epsilon_0 c}\right)}{\left|\frac{n_1\cos\theta_2 + n_2\cos\theta_1}{2} + \frac{\sigma_N}{2\epsilon_0 c}\cos\theta_1\cos\theta_2\right|^2}, \tag{11}$$

where θ_2 is the refracted angle. The above enounced impedance matching conditions have to be changed accordingly:

$$\begin{aligned} \mathrm{Re}\,(\sigma_N/\epsilon_0 c)_s &= n_1\cos\theta_1 + n_2\cos\theta_2, \\ \mathrm{Re}\,(\sigma_N/\epsilon_0 c)_p &= \frac{n_1\cos\theta_2 + n_2\cos\theta_1}{\cos\theta_1\cos\theta_2}, \end{aligned} \tag{12}$$

while the condition on the imaginary part of the conductivity stays the same for both polarizations.

In Fig. 3(a) the relations (6)–(8) are plotted for s polarization and a emergence medium refractive index $n_2 = 0.1$. Absorption is still quite high (i.e., above 90%) at low angles and reaches exactly 100% at the value of the critical angle $\theta_L = a\sin(n_2/n_1)$ for total internal refraction. It is easy to demonstrate that at this particular angle $\theta_L \approx n_2$ with n_2 approaching zero. It implies that $\cos\theta_L \approx 1$ and that $A \approx 1$ when $\mathrm{Re}(\sigma_N/\varepsilon_0 c) = n_1$, the impedance matching condition. At higher incident angle, the impedance matching condition is no longer fulfilled and the absorption decreases progressively. Transmittance is uniformly zero above the critical angle θ_L as expected. The corresponding absorption map [Fig. 3(b)] clearly indicates a zone of very high absorption ($A > 90\%$) for vanishing refractive index n_2. The dotted blue line indicates the critical angle θ_L for the refractive index varying continuously from $n_2 = 0.001$ to 2. In p polarization, at critical angle θ_L, reflectance is identically equal to one, whatever the refractive index of the emergence medium [Figs. 3(c) and 3(d)]. However, the Brewster angle $\theta_B = a\tan(n_2/n_1)$ is degenerate with the critical angle θ_L when the refractive index of the emergence medium approaches zero, i.e., $\theta_B \approx a\tan(n_2/n_1) \approx a\sin(n_2/n_1) \approx \theta_L$. This degenerescence creates a particular situation where both reflectance and transmittance are equal to zero above the critical angle. It yields perfect absorption in those conditions. Once the incident angle increases, the impedance matching condition for p polarization is not fulfilled anymore and reflectance increases. Consequently, absorption presents quite high values

for such a device ($A > 90\%$ for nonpolarized radiations and $\theta_1 > 45$ deg).

IV. CASE OF A FINITE SLAB OF EPSILON-NEAR-ZERO METAMATERIAL

The upon quest for perfect absorption was developed for a semi-infinite emergence medium. However, this situation is not likely to happen in real life applications. Let us consider the same structure as described above (Fig. 1) with a slab of finite thickness d over which N graphene/PMMA units are deposited. Analytical formulations for reflectance, transmittance, and absorption are consequently affected by the introduction of this extra-parameter d and read, for normal incidence,

$$R_{\text{slab}} = \frac{(\varepsilon_2+1)^2 + (1+a^2)(\sigma_N/\varepsilon_0 c)^2 + 2(\sigma_N/\varepsilon_0 c)(\varepsilon_2-1) - 4\varepsilon_2}{(\varepsilon_2+1+\sigma_N)^2 + a^2(\sigma_N/\varepsilon_0 c+2)^2}, \tag{13}$$

$$T_{\text{slab}} = \frac{4(a^2+\varepsilon_2)}{(\varepsilon_2+1+\sigma_N/\varepsilon_0 c)^2 + a^2(\sigma_N/\varepsilon_0 c+2)^2}, \tag{14}$$

$$A_{\text{slab}} = \frac{4(\sigma_N/\varepsilon_0 c)(a^2+1)}{(\varepsilon_2+1+\sigma_N/\varepsilon_0 c)^2 + a^2(\sigma_N/\varepsilon_0 c+2)^2}, \tag{15}$$

with $a = \frac{n_2}{\tan(n_2 k_0 d)}$, k_0 is the wave vector in vacuum, and ε_2 is the electric permittivity of the substrate. Those relations are valid for air as incidence and emergence media. If the permittivity of the slab goes to zero, the parameter a reduces to $1/k_0 d$. Moreover, if the product $k_0 d$ is large enough, $a \ll 1$ and consequently, the above expression for absorption simplifies to $A_{\text{slab}} = \frac{4\sigma_N/\varepsilon_0 c}{(1+\sigma_N/\varepsilon_0 c)^2}$. The optimization of absorption as described earlier implies that the impedance matching conditions remain the same as Eq. (5), with n_2 equal to 0. Once those adjusted impedance matching conditions are fulfilled, absorption exactly equals 100% as expected.

However, the consequence of the optimization of the absorption of the different parameters, i.e., the thickness of the ENZ substrate, its refractive index, and the operating wavelength, makes them dependent from each other. As shown in Fig. 4, different combinations of thicknesses and refractive index lead to high absorption. Several modes occur in the absorption pattern. This stands for the thin film interference mechanism, since maximum absorption (dotted green line) is obtained according to the relation

$$d = \frac{\lambda}{4n_2} \tag{16}$$

and any odd integer multiple of it. Actually, this equation can also be retrieved by taking the minimum of the partial derivative $\partial A_{\text{slab}}/\partial a$ and corresponds to a quarter-wave blade. Perfect absorption with a slab of finite thickness (couple of centimeters) can then also be reached using 2D conducting materials and ENZ metamaterials, if its thickness verifies Eq. (16).

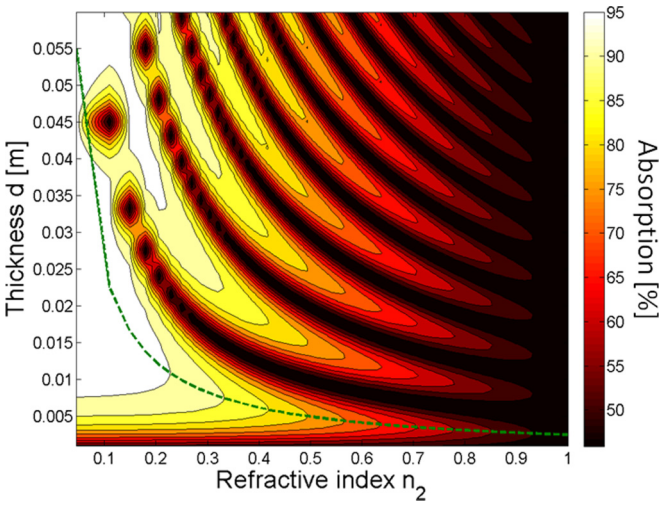

FIG. 4. Absorption of a graphene-PMMA heterostructure consisting of three PMMA/graphene units on a finite slab of thickness d as a function of thickness of the substrate d and its refractive index n_2. Refractive index n_2 varies from 0.04 to 1. Green dotted line indicates maximal absorption following interference theory.

V. DISCUSSION

The above developments present general cases of combinations of 2D materials and metamaterials to reach perfect absorption in a novel way. Though some comments can be made from the analytical derivations. As for all layered systems, the product $k_0 d$ is capital for governing the propagation of waves. If the refractive index n_2 vanishes, so does the wave vector via the dispersion relation. Moreover, when the thickness of the substrate is small compared to the wavelength, the fields will be perfectly transmitted (see Eq. (14) and Refs. [18,42] where ENZ material acts as perfect coupler between waveguides). In our case, this effect is undesired and the requirement of rather thick substrate hinders the ultrathin aspect of the device. However, since the proposed strategy to reach perfect absorption is general, moving towards shorter operating wavelengths is possible. This would permit us to further decrease the size of the total device. Nevertheless, graphene conductivity is lower in the visible regime, i.e., $\text{Re}(\sigma_{2D})/(\varepsilon_0 c) = \frac{e^2}{4\hbar\varepsilon_0 c} = 0.0229$ if $\hbar\omega > 2E_F$ with e, the elementary electric charge [43]. From the relation $\sigma_N = N\sigma_{2D}$, it will require either about 45 graphene layers or using another highly conducting 2D material to retrieve perfect absorption. The first solution is not realistic from an experimental point of view and the second one might not exist for visible light with conventional conducting materials.

The real character of graphene conductivity and its small variation with frequency below 100 GHz [35,44] insures absorption on a broadband range of em frequencies. A broadband ENZ metamaterial is also necessary. Natural polaritonic materials such as LiF, KCl, or NaCl present ENZ characteristics in the THz domain [45–48]. Incident em waves excite and couple with optical phonons presenting a resonance in the THz regime. For example, KCl presents a ENZ response around 6 THz and a Drude-Lorentz model can be applied. Another strategy, in the optical domain, uses silica layers filled with Ag inclusions of different filling factors and different thicknesses to reach ENZ between 630 and 680 nm [49]. However, as proved in the above considerations, an exactly zero refractive index is not required. Values smaller than 0.2 are still sufficient for obtaining quite high, but not perfect, absorption and the range of frequencies verifying the impedance matching conditions is broader.

In conclusion, the present work shows the possibility to reach perfect absorption using any kind of dissipative 2D material and an ENZ metamaterial serving as substrate. Analytical formulations for reflectance, transmittance, and absorbance are derived for the case of semi-infinite and finite ENZ metamaterial substrates, both presenting perfect absorption property once impedance matching conditions are fulfilled. The ENZ metamaterial hinders the radiation to go through the substrate and forces it to be dissipated in the absorbing 2D material. Specifically, three graphene layers can perfectly absorb incoming radiations at 30 GHz if it lies on a thick ENZ metamaterial. Angular robustness is demonstrated for near-zero refractive index semi-infinite emergence medium. A degenerescence between the critical angle for total internal refraction and Brewster angle is evidenced calling for a particular state of perfect absorption. This proposed strategy can be applied to other operating wavelengths or other emerging 2D material in order to build efficient shielding devices.

ACKNOWLEDGMENTS

Helpful discussion with N. Engheta is greatly appreciated. The research leading to this work has received funding from the European Union H2020 Program under Grant Agreement No. 649953 “Graphene-Driven Revolutions in ICT and Beyond” and Grant Agreement No. 318617 Marie Curie International Research Staff Exchange Scheme Fellowship (MC-IRSES FAEMCAR project). This research used resources of the “Plateforme Technologique de Calcul Intensif (PTCI)” (http://www.ptci.unamur.be) located at the University of Namur, Belgium, which is supported by the F.R.S.-FNRS under the convention No. 2.5020.11. The PTCI is member of the “Consortium des quipements de Calcul Intensif (CÉCI)” (http://www.ceci-hpc.be).

[1] C. R. Paul, *Introduction to Electromagnetic Compatibility* (John Wiley and Sons, Hoboken, NJ, 2006), p. 980.
[2] O. Balci, E. O. Polat, N. Kakenov, and C. Kocabas, Nat. Commun. **6**, 6628 (2015).
[3] B. Wu, H. M. Tuncer, M. Naeem, B. Yang, M. T. Cole, W. I. Milne, and Y. Hao, Sci. Rep. **4**, 4130 (2014).
[4] K. S. Novoselov, V. I. Falko, L. Colombo, P. R. Gellert, M. G. Schwab, and K. Kim, Nature (London) **490**, 192 (2012).
[5] S. Bae, H. Kim, Y. Lee, X. Xu, J.-S. Park, Y. Zheng, J. Balakrishnan, T. Lei, H. Ri Kim, Y. I. Song, Y.-J. Kim, K. S. Kim, B. Ozyilmaz, J.-H. Ahn, B. H. Hong, and S. Iijima, Nat. Nano **5**, 574 (2010).
[6] K. Batrakov, P. Kuzhir, S. Maksimenko, A. Paddubskaya, S. Voronovich, P. Lambin, T. Kaplas, and Y. Svirko, Sci. Rep. **4**, 7191 (2014).
[7] K. Batrakov, P. Kuzhir, S. Maksimenko, N. Volynets, S. Voronovich, A. Paddubskaya, G. Valusis, T. Kaplas, Yu. Svirko, and Ph. Lambin, Appl. Phys. Lett. **108**, 123101 (2016).
[8] H. H. Kim, S. K. Lee, S. G. Lee, E. Lee, and K. Cho, Adv. Funct. Mater. **26**, 2070 (2016).
[9] M. Lobet, N. Reckinger, L. Henrard, and P. Lambin, Nanotechnology **26**, 285702 (2015).
[10] J. B. Pendry, Phys. Rev. Lett. **85**, 3966 (2000).
[11] S. Foteinopoulou, E. N. Economou, and C. M. Soukoulis, Phys. Rev. Lett. **90**, 107402 (2003).
[12] V. M. Shalaev, Nat. Photon **1**, 41 (2007).
[13] J. B. Pendry, Science **306**, 1353 (2004).
[14] J. B. Pendry, D. Schurig, and D. R. Smith, Science **312**, 1780 (2006).
[15] U. Leonhardt, Science **312**, 1777 (2006).
[16] N. Fang, H. Lee, C. Sun, and X. Zhang, Science **308**, 534 (2005).
[17] S. Zhong, Y. Ma, and S. He, Appl. Phys. Lett. **105**, 023504 (2014).
[18] M. Silveirinha and N. Engheta, Phys. Rev. Lett. **97**, 157403 (2006).
[19] X. Huang, Y. Lai, Z. H. Hang, H. Zheng, and C. T. Chan, Nat. Mater **10**, 582 (2011).
[20] P. Moitra, Y. Yang, Z. Anderson, I. I. Kravchenko, D. P. Briggs, and J. Valentine, Nat. Photon **7**, 791 (2013).
[21] Y. Li, S. Kita, P. Munoz, O. Reshef, D. I. Vulis, M. Yin, M. Loncar, and E. Mazur, Nat. Photon **9**, 738 (2015).
[22] S. Feng and K. Halterman, Phys. Rev. B **86**, 165103 (2012).
[23] M. A. Badsha, Y. C. Jun, and C. K. Hwangbo, Opt. Commun. **332**, 206 (2014).
[24] J. Yoon, M. Zhou, M. A. Badsha, T. Y. Kim, Y. C. Jun, and C. K. Hwangbo, Sci. Rep. **5**, 12788 (2015).
[25] T. S. Luk, S. Campione, I. Kim, S. Feng, Y. C. Jun, S. Liu, J. B. Wright, I. Brener, P. B. Catrysse, S. Fan, and M. B. Sinclair, Phys. Rev. B **90**, 085411 (2014).
[26] S. Lee, T. Q. Tran, M. Kim, H. Heo, J. Heo, and S. Kim, Opt. Express **23**, 33350 (2015).
[27] This numerical technique considers graphene as a one-atom-thick layer of thickness 0.34 nm [29,31]. This distance corresponds to the interlayer separation of graphite.
[28] M. G. Moharam and T. K. Gaylord, J. Opt. Soc. Am. **71**, 811 (1981).
[29] M. Lobet, M. Sarrazin, F. Cecchet, N. Reckinger, A. Vlad, J.-F. Colomer, and D. Lis, Nano Lett. **16**, 48 (2016).
[30] R. Kotsilkova, P. Todorov, E. Ivanov, T. Kaplas, Y. Svirko, A. Paddubskaya, and P. Kuzhir, Carbon **100**, 355 (2016).

[31] F. J. Garcia de Abajo, ACS Photon. **1**, 135 (2014).
[32] F. H. L. Koppens, D. E. Chang, and F. J. Garcia de Abajo, Nano Lett. **11**, 3370 (2011).
[33] L. A. Falkovsky, J. Phys.: Conf. Ser. **129**, 012004 (2008).
[34] N. Mermin and D. Lindhard, Phys. Rev. B **1**, 2362 (1970).
[35] N. Rouhi, D. Jain, S. Capdevila, L. Jofre, E. Brown, and P. J. Burke, in *11th IEEE Conference on Nanotechnology (IEEE-NANO)* (IEEE, Portland, Oregon, New York, 2011), pp. 1205–1207.
[36] N. Petrone, C. R. Dean, I. Meric, A. M. van der Zande, P. Y. Huang, L. Wang, D. Muller, K. L. Shepard, and J. Hone, Nano Lett. **12**, 2751 (2012).
[37] J. W. Lamb, Int. J. Infrared Milli. Waves **17**, 1997 (1996).
[38] H. Bosman, Y. Y. Lau, and R. M. Gilgenbach, Appl. Phys. Lett. **82**, 1353 (2003).
[39] N. Engheta, in *IEEE Antennas and Propagation Society International Symposium* (IEEE, San Antonio, Texas, New York, 2002), Vol. 2, pp. 392–395.
[40] S. A. Tretyakov and S. I. Maslovski, Microwave Opt. Technol. Lett. **38**, 175 (2003).
[41] R. L. Fante and M. T. McCormack, IEEE Trans. Antennas Prop. **36**, 1443 (1988).
[42] R. Liu, Q. Cheng, T. Hand, J. J. Mock, T. J. Cui, S. A. Cummer, and D. R. Smith, Phys. Rev. Lett. **100**, 023903 (2008).
[43] R. R. Nair, P. Blake, A. N. Grigorenko, K. S. Novoselov, T. J. Booth, T. Stauber, N. M. R. Peres, and A. K. Geim, Science **320**, 1308 (2008).
[44] J. D. Buron, F. Pizzocchero, B. S. Jessen, T. J. Booth, P. F. Nielsen, O. Hansen, M. Hilke, E. Whiteway, P. U. Jepsen, P. Boggild, and D. H. Petersen, Nano Lett. **14**, 6348 (2014).
[45] A. A. Basharin, M. Kafesaki, E. N. Economou, and C. M. Soukoulis, Opt. Express **20**, 12752 (2012).
[46] M. Massaouti, A. A. Basharin, M. Kafesaki, M. F. Acosta, R. I. Merino, V. M. Orera, E. N. Economou, C. M. Soukoulis, and S. Tzortzakis, Opt. Lett. **38**, 1140 (2013).
[47] E. D. Palik, *Handbook of Optical Constants of Solids* (Academic, Burlington, VT, 1997), pp. 675–693, 703–718.
[48] J. E. Eldridge and E. D. Palik, in Ref. [47], pp. 775–793.
[49] L. Sun, K. W. Yu, and X. Yang, Opt. Lett. **37**, 3096 (2012).